El Niño effects in the Palmyra Atoll region: oceanographic changes and bigeye tuna (*Thunnus obesus*) catch rate variability

EVAN A. HOWELL[1]* AND DONALD R. KOBAYASHI[1,2]

[1]*Ecosystems and Oceanography Division, Pacific Islands Fisheries Science Center, NMFS, NOAA, 2570 Dole Street, Honolulu, HI 96822, USA*
[2]*Department of Environmental Sciences, University of Technology, Sydney, Broadway, NSW, Australia*

ABSTRACT

A generalized additive model (GAM) was constructed to separate and quantify the effects of fishery-based (operational) and oceanographic parameters on the bigeye tuna (*Thunnus obesus*) catch rates at Palmyra Atoll in the central Tropical Pacific. Bigeye catch, the number of hooks per set, and set location from 4884 longline sets spanning January 1994 to December 2003 were used with a temporally corresponding El Niño-Southern Oscillation (ENSO) indicator built from sea surface height (SSH) data. Observations of environmental data combined with the results from the GAM indicated that there is an increase in bigeye catch rates corresponding to an increase in eastward advection during the winter months of El Niño events. A seasonal pattern with higher bigeye catch rates from December to April and a spatial pattern with higher rates to the northeast and northwest of the atoll were observed during this study period. It is hypothesized that the combination of the eastward advection of the warm pool coupled with vertical changes in temperature during the winter months of El Niño events increases the availability of bigeye tuna in this region. This increase in availability may be due to a change in exploitable population size, location, or both.

Key words: bigeye tuna, El Niño, empirical orthogonal function, fishery oceanography, generalized additive model, Palmyra Atoll

INTRODUCTION

Palmyra Atoll, in the central Tropical Pacific, is roughly 960 nautical miles south of Honolulu, Hawaii. This region is situated close to the convergence area between the warm, less saline western waters (warm pool) and the cold, more saline eastern water (cold tongue) with climate dominated by El Niño-Southern Oscillation (ENSO) events. The Hawaiian longline fishery operates mainly in the central Pacific Ocean targeting swordfish (*Xiphias gladius*), bigeye tuna (*Thunnus obesus*), and yellowfin tuna (*Thunnus albacares*) and since 1998 much effort has been directed at the area around Palmyra Atoll. The species composition of the catch in this region is dominated by yellowfin tuna and higher market value bigeye tuna (Ito and Machado, 1999), with observed large interannual variability of both species. The appearance of ENSO results in large-scale oceanographic fluctuations with a shift of the convergence zone to the east of Palmyra Atoll during El Niño (warm) and to the west during La Niña (cold) events (Picaut *et al.*, 1996). The effect of ENSO-induced oceanographic fluctuations on the migration of tuna throughout the Pacific has been well documented (Lehodey *et al.*, 1997, 1998; Polovina *et al.*, 2001), with skipjack tunas in the equatorial areas following the east–west movement of the warm-pool/cold-tongue convergence zone, yet the importance of ENSO on bigeye tuna is not well documented for this region.

Generalized additive models (GAMs) are a relatively new analytical technique (Hastie and Tibshirani, 1990) and have been utilized in previous fishery studies involving fish surveys (Swartzman *et al.*, 1992), catch rates (catch per set) (Walsh and Kleiber, 2001; Walsh *et al.*, 2002), and catch-per-unit-effort (CPUE) (Bigelow *et al.*, 1999). We use a GAM to quantify and describe the effects of fisheries operational and oceanographic variables on bigeye catch rates in the Palmyra Atoll area from 1994 to 2003. A descriptive model of bigeye tuna catch in the Palmyra Atoll region would help in understanding the effects of El Niño on the regional oceanography and their relationship to longline fishery dynamics in

*Correspondence. e-mail: Evan.Howell@noaa.gov
Received 19 January 2005
Revised version accepted 17 August 2005

 doi:10.1111/j.1365-2419.2005.00397.x

this apparently productive but remote and dynamic area.

DATA AND METHODS

Longline fishery data

Hawaii-based longline fishing activity from January 1994 through September 2003 was examined using the federally mandated longline logbook data provided by the Fishery Monitoring and Economics Program (FMEP) of the National Marine Fisheries Service (NMFS), and Pacific Islands Fisheries Science Center (PIFSC). Logbook data were parsed to provide records of longline fishing sets within the Palmyra Atoll region (158–167°W, 4–9°N) (Fig. 1). A total of 4884 longline sets were deployed in the Palmyra region from 1994 through 2003. Previous work to assess the accuracy of bigeye catch data in the federal logbooks reported that approximately 90% of longline sets had an error of ±2 fish reported when compared to the federally mandated longline observer data set ($r^2 = 0.941$; Walsh, 2000). Correlations were also high for set month ($r^2 = 0.954$), the number of hooks ($r^2 = 0.91$), latitude ($r^2 = 0.997$), and longitude ($r^2 = 0.989$; Walsh, NMFS, Hawaii, personal communication). Nominal CPUE was plotted to show the temporal variability in catch rates without the effect of any change in the number of hooks per set. We calculated the nominal CPUE for each set by

$$\mathrm{CPUE} = \frac{(k+d)}{n}, \qquad (1)$$

where k is the number of kept bigeye tuna per set, d the number of discarded bigeye tuna per set, and n is the hooks per set. The fishery-dependent predictor variables used in the model were all taken as the corresponding value for each particular set. Historically, a suite of longline predictors including the date of set, latitude, longitude, number of hooks, set time, and number of light sticks per hook (Bigelow *et al.*, 1999; Walsh *et al.*, 2002) have been used to build a descriptive model. Attempting to use all of the available information in addition to our environmental data would result in a model susceptible to correlation effects and overparameterization, in addition to decreasing the model's predictive power. To avoid these problems and to keep the model as parsimonious as possible, certain fishery-based predictors were discarded. The number of light sticks is a useful parameter in most studies, yet 98.5% of our study sets reported zero light sticks. The time the gear was set (set time) was not used because 89.5% of the sets were initiated in the limited time window between 0600 and 0900 (i.e., daytime sets). The model also found these two predictors to be unimportant. Four fishery-dependent predictor variables were used in the model. Set month corresponded to the month of the hauling of the gear, set number of hooks was the number of hooks deployed per set, and the set latitude and longitude values were the average value of the setting and the hauling of the gear.

Environmental predictor data

Sea surface height (SSH) data were mapped at a global 0.3° by 0.3° resolution with orbit error reduction provided by the Ssalto program of the Centre National d'études Spatiales, France. This altimetry product is a weekly average of the measured along-track sea-level profiles mapped to a mercator projection. The average of these along-track profiles from 1993 to 1998 was used to create a mean profile that was then subtracted from the mapped product to obtain the sea-level anomalies. For the time period October 1992 to July 2002 data from the TOPEX/POSEIDON altimeter were used. After July 2002 JASON-1 was put into operation along the same orbit as TOPEX/POSEIDON, and from this date forward its data were used in the study. To compute the geostrophic currents, the 1994 NODC World Ocean Atlas Levitus long-term mean 1000-m dynamic height data set was added to the SSH anomaly files to create an 'absolute' SSH. The east–west (x) and north–south (y) gradients, $\frac{dz}{dx}$ and $\frac{dz}{dy}$, were derived from this height (z) and subsequently used to calculate the east–west (u) and north–south (v) components of the geostrophic current, as described by Polovina *et al.* (1999).

Subsurface temperature data used in this study were collected by ATLAS buoys within the Tropical Atmosphere-Ocean (TAO) program. TAO subsurface temperature data were measured by thermistors at constant depths moored to buoys at specific locations in the equatorial Pacific. Data were delivered at a rate of 1–10 samples per minute and averaged to a daily value. The depth of the 20°C isotherm is calculated from temperature profiles using linear interpolation of depth versus temperature.

Figure 1. (a) The total number of hooks set in the Hawaii-based longline fishery from 1994 to 2003. (b) Total hooks set in the Palmyra region from 1994 to 2003. In both figures data were resampled to 1° × 1° grid points and cells with less than three total sets were deleted to maintain confidentiality.

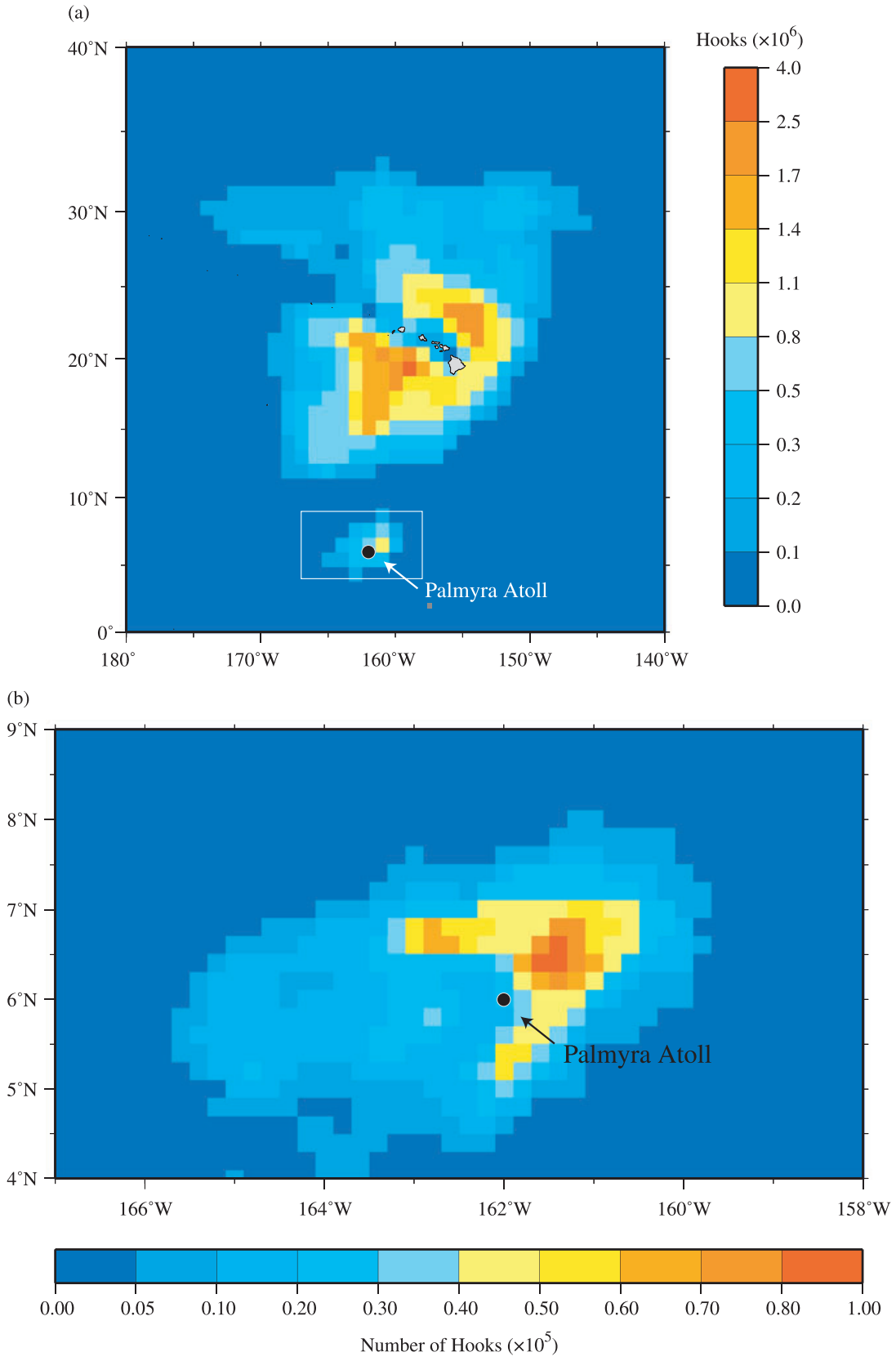
(a)
40°N
30°N
20°N
10°N
0°
180°
170°W
160°W
150°W
140°W
Hooks (×10^6)
4.0
2.5
1.7
1.4
1.1
0.8
0.5
0.3
0.2
0.1
0.0
Palmyra Atoll
(b)
9°N
8°N
7°N
6°N
5°N
4°N
166°W
164°W
162°W
160°W
158°W
Palmyra Atoll
0.00
0.05
0.10
0.20
0.30
0.40
0.50
0.60
0.70
0.80
1.00
Number of Hooks (×10^5)

Empirical orthogonal function analysis

Empirical orthogonal function (EOF) analysis was performed to construct an indicator of ENSO activity in the equatorial region on the SSH data set from 1994 to 2003. This technique has been previously described in detail (Polovina and Howell, 2005), and a shortened form is included here for descriptive purposes. The time series of monthly SSH was detrended and standardized by removing the average monthly signal and subtracting the long-term mean. Land values were removed to create the final detrended matrix $F(x,t)$, which was then decomposed using the form

$$F(x,t) = \sum_{i=1}^{N} a_i(t)\phi_i(x), \quad (2)$$

where $a_i(t)$ are the principal components (PCs) (temporal expansion coefficients) of the spatial components $\phi_i(x)$ (Wilson and Adamec, 2001). This analysis results in N statistical modes, each with a vector of PC expansion coefficients a_i and a corresponding spatial component map ϕ_i. Each of these maps represents a standing oscillation, and the expansion coefficients represent how this pattern oscillates through time. These modes are orthogonal and by definition uncorrelated with each other. EOF analysis is a purely statistical technique and there is no reason for the basis functions to be associated with physical forcings, yet the first modes often correspond to underlying processes (Uddstrom and Oien, 1999).

Generalized additive models

A GAM is a generalized linear model (GLM) in which the linear predictor is given by a user-specified sum of smooth functions of the covariates plus a conventional parametric component of the linear predictor (Wood, 2000). GAMs are useful when the predictor variables have non-linear effects upon the response variable. For example, longline catch rates have been shown to be strongly influenced by many different biological, environmental, and operational characteristics, often with highly non-linear effects (e.g., Bigelow *et al.*, 1999; Walsh and Kleiber, 2001; Walsh *et al.*, 2002). Some variables relate to catchability (e.g., gear performance), while others may relate to availability (e.g., fish abundance/seasonality). These effects are considered additive, and the GAM can be used to predict bigeye catch rates given a set of predictor variables for a particular set of longline fishing gear.

GAMs were constructed in the R programming environment using the *gam* function of the *mgcv* package (Wood, 2000). Model building was done manually to avoid problems that can arise in automated selection procedures (Harrell, 2001). The GAMs were fit in the form

$$g(u_i) = \beta_0 + s_1(x_{1i}) + s_2(x_{2i}) + \cdots s_n(x_{ni}), \quad (3)$$

where g is the link function, u_i the expected value of the dependent variable (here bigeye catch per set), β_0 is a constant, and each s_n is a smooth function of covariate x_n. Catch rates follow a continuous distribution so we chose Gaussian as the family, which is associated with an identity link function. The catch rate data were log transformed to keep variance constant. To account for zero catch-rate values, a value of 1 was added to all sets before the log transformation. A normal probability plot of the cumulative distribution of the residuals indicates that our assumption of a Gaussian distribution was appropriate. The smooth functions were penalized thin plate splines, which allow for ease in model selection from the generalized cross-validation (GCV) score (analogous to the Akaike information criterion), which is defined as

$$\mathrm{GCV} = \frac{nD}{(n-df)^2}, \quad (4)$$

where n is the number of samples, D the deviance, and df is the effective degrees of freedom of the model. The final model using the five predictors described previously was of the form

$$E[\log_e(\mathrm{Bigeye}+1)] = \beta_0 + s(\mathrm{Month}) + s(\mathrm{Numhooks}) + s(\mathrm{EOF}) + s(\mathrm{Lon, Lat}), \quad (5)$$

where the four fishery dependent predictors were as previously described and EOF referring to the PC time series of the empirical orthogonal analysis on SSH. All predictors were modeled as continuous variables. The dependence on spatial location was modeled as a bivariate function of longitude and latitude rather than summing the univariate effects of these two variables, as suggested by Wood and Augustin (2002).

RESULTS

Fishery variability

Minimal longline effort took place in the Palmyra Atoll area before 1998, followed by an increase in the amount of hooks set from 1998 to 2003 (Fig. 2). The percentage of hooks in the entire Hawaii-based longline fishery set in the Palmyra region each year followed a similar trend (Fig. 2). An average of 1.6% of the total hooks set was in this area before 1998, 10.0% in 1998, and an average of 7.4% from 1999 to 2002. Less than 1% of the total effort was in the Palmyra region in 2003. Most trips and corresponding sets

Figure 2. Annual effort for the Palmyra region by quarter. The annotation above the bars represents the percentage of effort set in this region for the entire longline fishery.

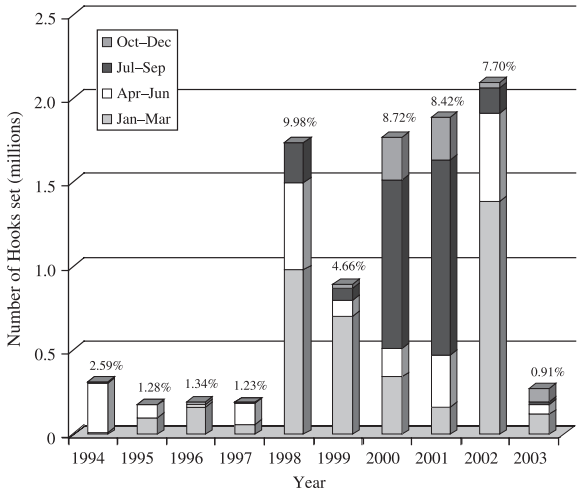

occur in the first half of the year, with an exception in 2000–01 where over 50% of the effort was in the third quarter (Fig. 2). In all years less than 15% of the fourth quarter effort occurs in this region. Spatially, historical effort from 1994 to 2003 was broad across the area with a high concentration of effort to the north, east, and northeast of the atoll (Fig. 1b).

The annual CPUE values for bigeye tuna in the Palmyra region are shown in Fig. 3a. Values were moderate prior to 1998, high in 1998 (18.9% of all bigeye caught in the fishery), declined from 1999 to 2001, and were at moderate levels during 2002 and 2003. A time series of the monthly CPUE values is plotted to assess the seasonal variability (Fig. 3b). Moderate CPUE values were found for the first two quarters (January–June) in all years, with a slight decline in 1999–01. CPUE values remained high throughout the first three quarters (January–September) of 1998 but were moderate in 2002. The highest bigeye CPUE values for the region were found in the first quarters of 1998 and 2003, years of strong and moderate El Niño conditions, respectively.

Environmental variability

The area around the Palmyra region is heavily affected by ENSO events on varying interannual scales. Time-series diagrams of the depths of the 20°C isotherm (here used as a proxy for thermocline depth), interpolated from individual TAO buoys on each of the four corners of the Palmyra region, are shown in Fig. 4. The depth of this feature at 8°N, 170°W was between 90 and 160 m and was slightly shallower during the 1994–95 and 2002–03 El Niño events. A slight decrease was observed during the La Niña period from 1998 to 2002 following the large signal jump from the 1997 to 1998 El Niño. The depth of the 20°C isotherm appeared to have more interannual variability at 8°N, 155°W, with depths ranging from 60 to 160 m. Signal increases were observed during the three El Niño events during the study, with a larger signal increase (shoaling of the isotherm) in the 1997–98 El Niño than the 1994–95 and 2002–03 events. The 20°C isotherm at 5°N, 170°W was on average deeper than at both northern locations, with depths ranging from 110 to 220 m. There was more intra-annual variability at this location which masked any El Niño effects other than the slight increase observed during 1997–98. The isotherm at 5°N, 155°W was slightly shallower than at 5°N, 170°W, with depths ranging from 80 to 220 m. Intra-annual variability again dominated the signal with slight shoaling of the isotherm during the 1997–98 El Niño event. These data show that the isotherm across the Palmyra region had a vertical gradient from west (deeper) to east (shallower) and from south (deeper) to north (shallower). During El Niño events the vertical gradient increased from 5 to 8°N with an overall rise of up to 70 m at 8°N during 1997–98. This spatial gradient and its effect on the distribution of bigeye catch during the 1997–98 El Niño are shown in Fig. 5. Satellite imagery of SSH and calculated geostrophic currents show the high gradients between 5 and 8°N during this time period. Strong eastward flow is observed at 6°N during January, 1998 (Fig. 5a) with two large cold core eddy features centered between 8 and 10°N which corresponded to a shoaling of the thermocline captured in the 20°C isotherm time series at 8°N. Through the next 5-month period (Fig. 5b–f) the reversal of the current system is evident, with an inversion of the SSH gradients and a movement of the bigeye catch locations to the west. As the current reversed a warm core eddy feature developed (Fig. 5d) which appeared to constrain the bigeye catch to this region north of Palmyra Atoll. This feature moved slightly east in May 1998 (Fig. 5e), and by June 1998 the reversal to westward flow from La Niña conditions was complete with minimal bigeye catch in this region.

EOF analysis of the monthly SSH shows the scope and changes in SSH over the entire equatorial region through time. The first mode of our EOF analysis described 36.7% of the variance in the system. ENSO events are marked by changes in the amplitude of the PC of the first mode of the SSH EOF for the equatorial

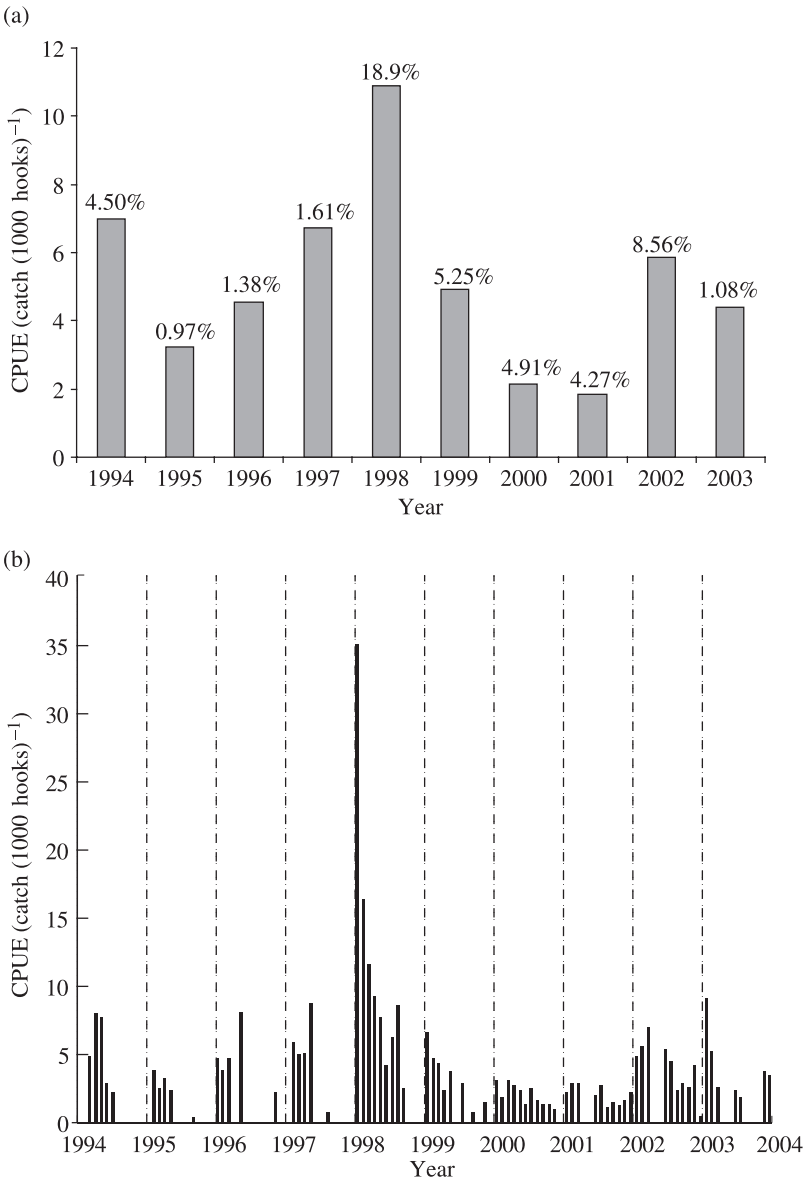

Figure 3. (a) Annual aggregated bigeye tuna CPUE for the Palmyra region. The annotation above the bars represents the percentage of bigeye tuna caught in this region for the entire longline fishery. (b) Monthly aggregated bigeye tuna CPUE for the Palmyra region. The dashed lines represent the first day of the first quarter. The dotted lines represent the first day of the second, third, and fourth quarters.

region (Fig. 6a). A positive trend in the PC is related to El Niño and a shift of the transport along the equator from westward to eastward. Negative amplitude is an indication of a shift in the current system from east to west during the start of La Niña conditions. There were signals indicating El Niño-like events in 1994–95, 1997–98, and 2002–03, with La Niña conditions in 1995–97 and 1998–02. The sea surface state can be reconstructed by taking the magnitude of the PC at each point in the time series and multiplying that across the spatial pattern (Fig. 6b). When the PC is positive the sea state is of the form shown in the spatial pattern, with the opposite pattern occurring during times when the PC is negative.

Generalized additive model

The results of our final five-predictor GAM are displayed in Table 1. All variables used were statistically significant ($P < 0.001$) when testing their exclusion from the model and decreased the GCV criterion. GAM results are presented in Fig. 7 and can be interpreted as the individual effect of a predictor variable on bigeye catch per set. The effect of month shows a seasonal cycle with higher bigeye catch rates in the months December to April, tapering down though the rest of the year (Fig. 7a). This seasonality in the fishery accounted for 21% of the cumulative variance explained (Table 1). The effect of effort on

Figure 4. Time series of the depth of the 20°C isotherm measured by the TAO array for (a) 8°N, 170°W; (b) 8°N, 155°W; 5°N, 170°W; 5°N, 155°W. The solid line in each graph represents a 2 month moving average.

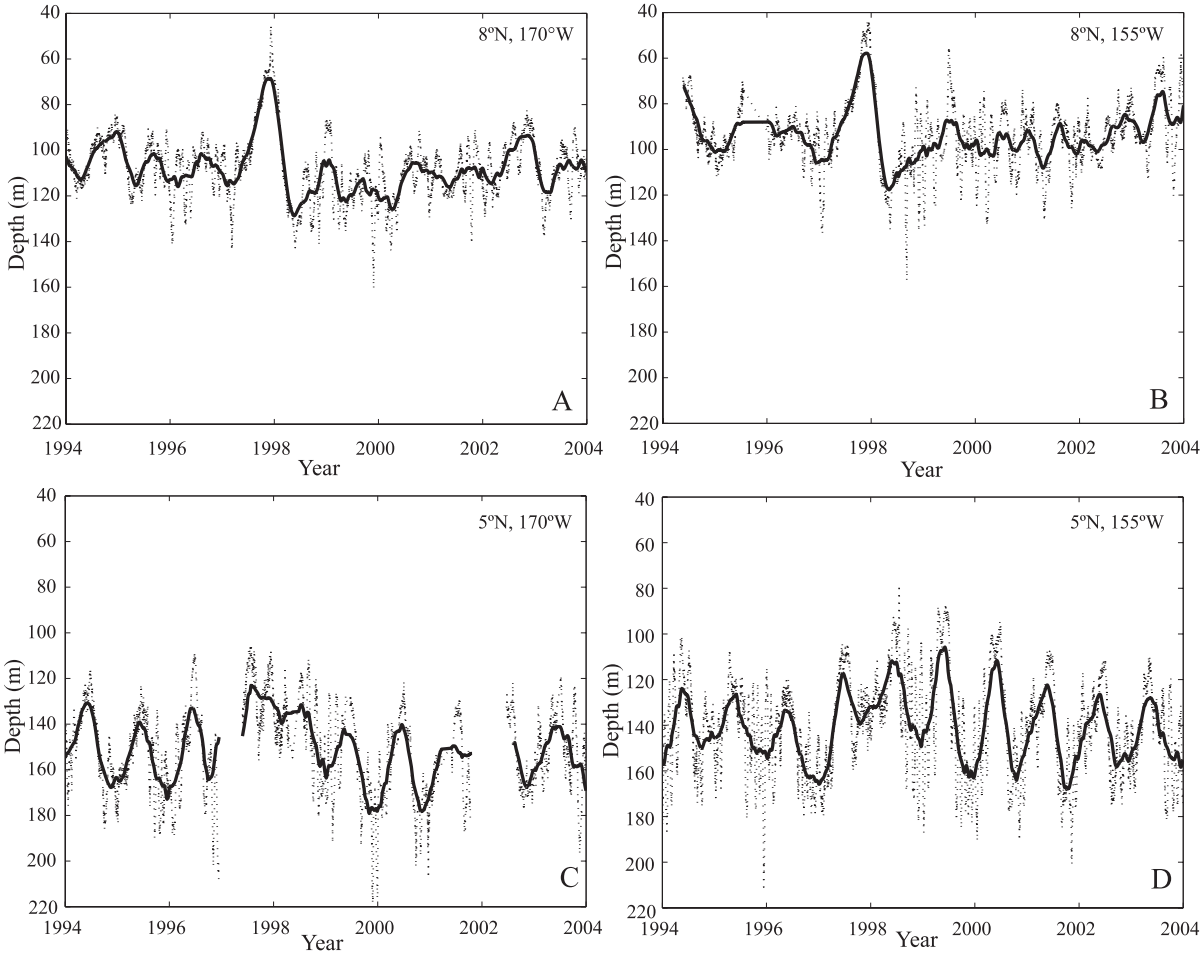

catch rates increases linearly for sets with less than 2000 hooks (7b), with a decrease in the slope in sets above this. There is a slight increase in the effect on sets with more than 3000 hooks but this is at the extremes of our data set, indicated by the large spread in our confidence intervals. This effect had less influence on the catch rates as reflected by the small increase in explained cumulative deviance and a small decrease in the residuals (Table 1). The effect of El Niño events on catch rates was captured in our EOF indicator variable, where large positive values reflect strong El Niño conditions in the study region and correspond to the highest effect on bigeye catch rates (Fig. 7c). This variable increased the explained cumulative deviance by 10% and resulted in a major reduction in the residuals (Table 1). The results from the modeled longitude–latitude interaction term (Fig. 7d) show the pattern of the spatial effect. High effects on catch rates were found to the northeast, northwest, and south of the atoll, with the northeast area corresponding to the area of highest historical effort. A low effect on catch rates was observed in the area immediately surrounding the atoll and zonally from 7 to 9°N. The results of the model fits can be seen in Fig. 8a. The correlation between each observed value and GAM prediction was $r^2 = 0.35$ ($N = 4844$) when computed on a set-by-set basis. For ease of interpretation, observed and GAM-derived sets were folded into monthly values. After this averaging, temporal patterns in the model's ability to fit became apparent while the correlation between the two data sets increased ($r^2 = 0.78$, Fig. 8a). A Q–Q plot of these monthly observed versus the monthly model predicted catch rates shows non-normality in the data extremes (Fig. 8b). The model overestimates sets with either no or low bigeye catch reported, while underestimating sets with higher than average ($\mu = 9.84$) bigeye caught per set.

Figure 5. SSH with geostrophic currents (vectors) for (a) January 1998; (b) February 1998; (c) March 1998; (d) April 1998; (e) May 1998; (f) June 1998. The black lines indicate the contour lines of the SSH with Levitus climatology added. The black circles represent the summation of bigeye catch per set in 1° × 1° cells. To maintain confidentiality cells with less than three total sets were removed. The black star represents Palmyra Atoll.

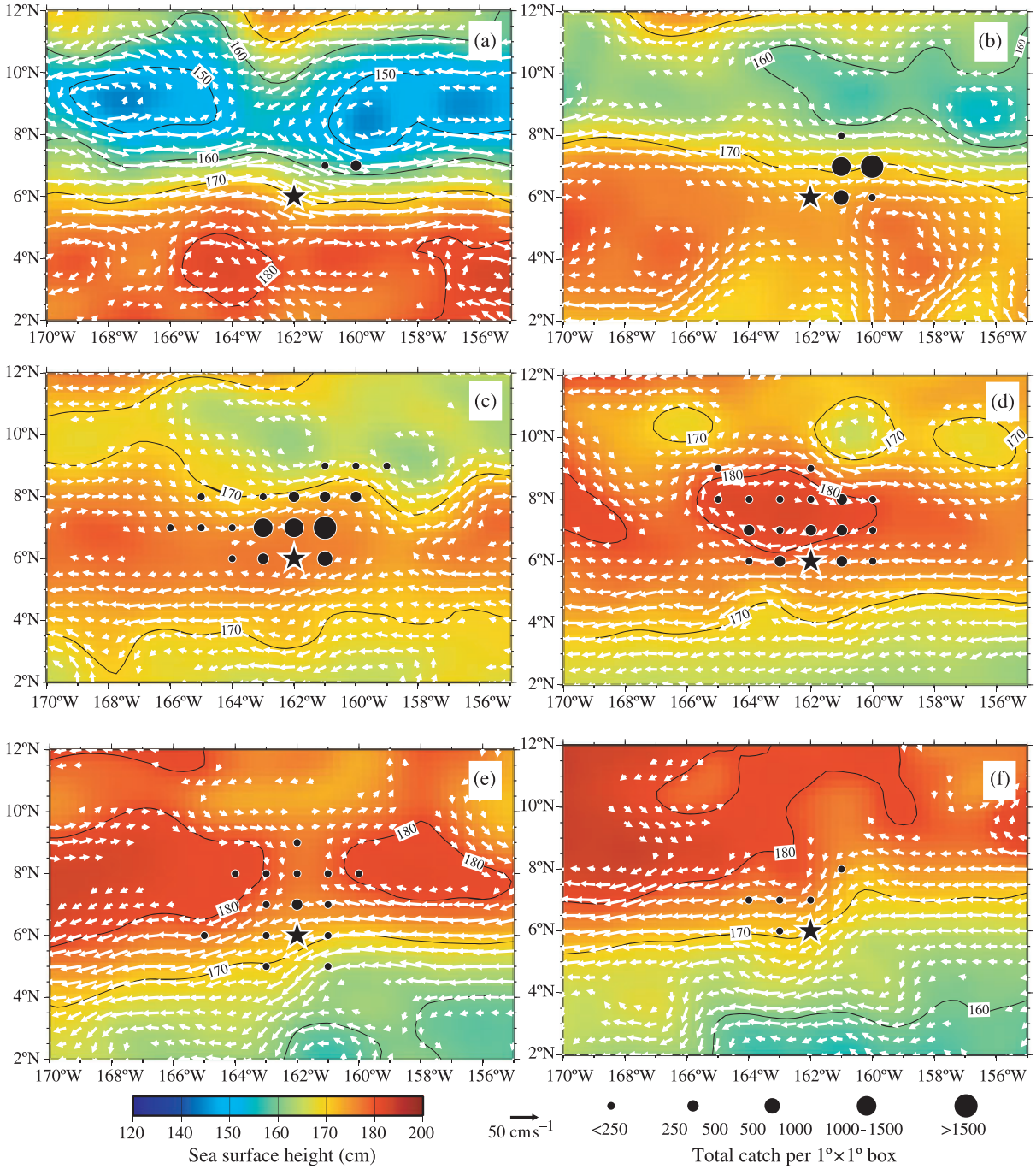

DISCUSSION

Results from the GAM show that the El Niño events are statistically important in generating high catch rates for the Hawaii-based longline fishery. The mechanism for this is more difficult to uncover, as El Niño effects may drive a vertical shift, a horizontal shift, or some combination of both in the distribution

Figure 6. (a) The PC of the first mode of the EOF analysis for the equatorial Pacific, which explained 36.17% of the total variance of the system. The gray-shaded areas represent El Niño events. (b) The spatial pattern for the EOF analysis. The black square represents the boundaries of the region of this study (158–167°W, 4–9°N).

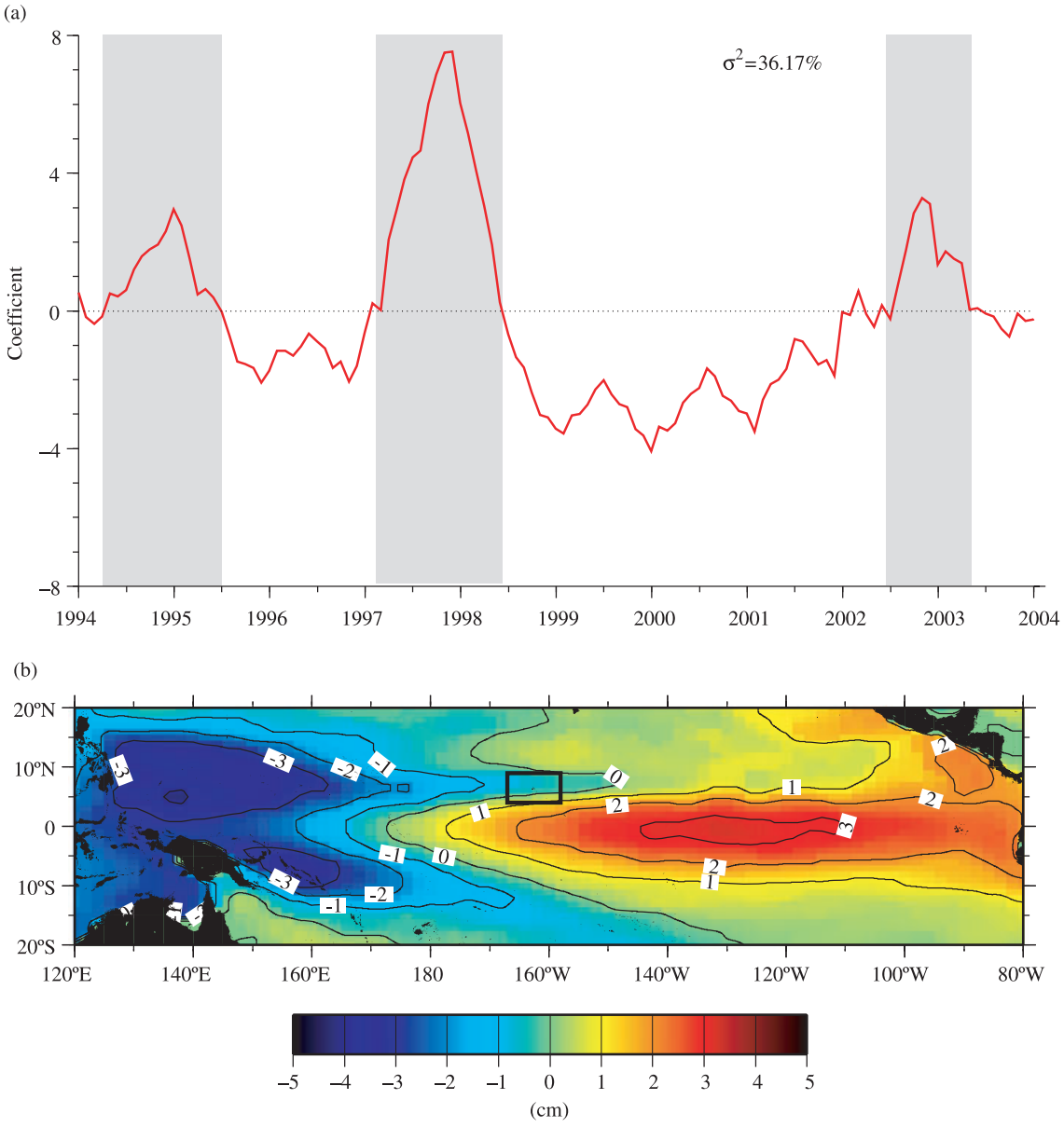

of bigeye tuna in the Palmyra region. The preferred habitat of bigeye tuna throughout the Pacific has been well studied (Hanamoto, 1987; Holland *et al.*, 1990; Boggs, 1992; Brill, 1994; Bigelow *et al.*, 2002; Musyl *et al.*, 2003), with bigeye generally caught in waters of about 8–15°C (100–400 m) (Hanamoto, 1987; Boggs, 1992). Oceanographic data show that the 1997–98 El Niño event altered the subsurface temperature in the area around Palmyra Atoll (Fig. 4). These changes in subsurface temperature would have altered the preferred habitat of bigeye tuna. The 50-m rise in the 20°C isotherm at 8°N during the 1997–98 El Niño may have allowed bigeye tuna to reach a cooler habitat at shallower depths. Oxygen data were not available, yet one possibility is that the shoaling of the subsurface waters also brings severely low oxygen waters closer to the surface during El Niño events. Bigeye tuna have strong thermoregulatory abilities and can withstand low oxygen levels for short periods of time (Brill, 1994),

Predictor variable	*df*	ΔGCV	ΔResiduals	*P* values	Cumulative deviance explained
Set month	5.63	0.865	3665.698	$<2.22 \times 10^{-16}$	21.40%
Set number of hooks	5.81	−0.011	−32.793	4.49×10^{-13}	22.60%
EOF	8.32	−0.104	−273.041	$<2.22 \times 10^{-16}$	32.30%
(Lon, Lat)	25.52	−0.038	−109.596	$<2.22 \times 10^{-16}$	36.40%

Table 1. Analysis of deviance of a five variable GAM of bigeye tuna catch rates (catch per set). ΔGCV represents the change in the GCV score.

Figure 7. The GAM-derived effect on bigeye tuna catch per set of (a): set month; (b): the number of hooks per set; (c): the PC time series of the EOF analysis on SSH; (d): the bivariate spatial (longitude–latitude) term. The color underlay represents the 1° × 1° grid of the historical effort.

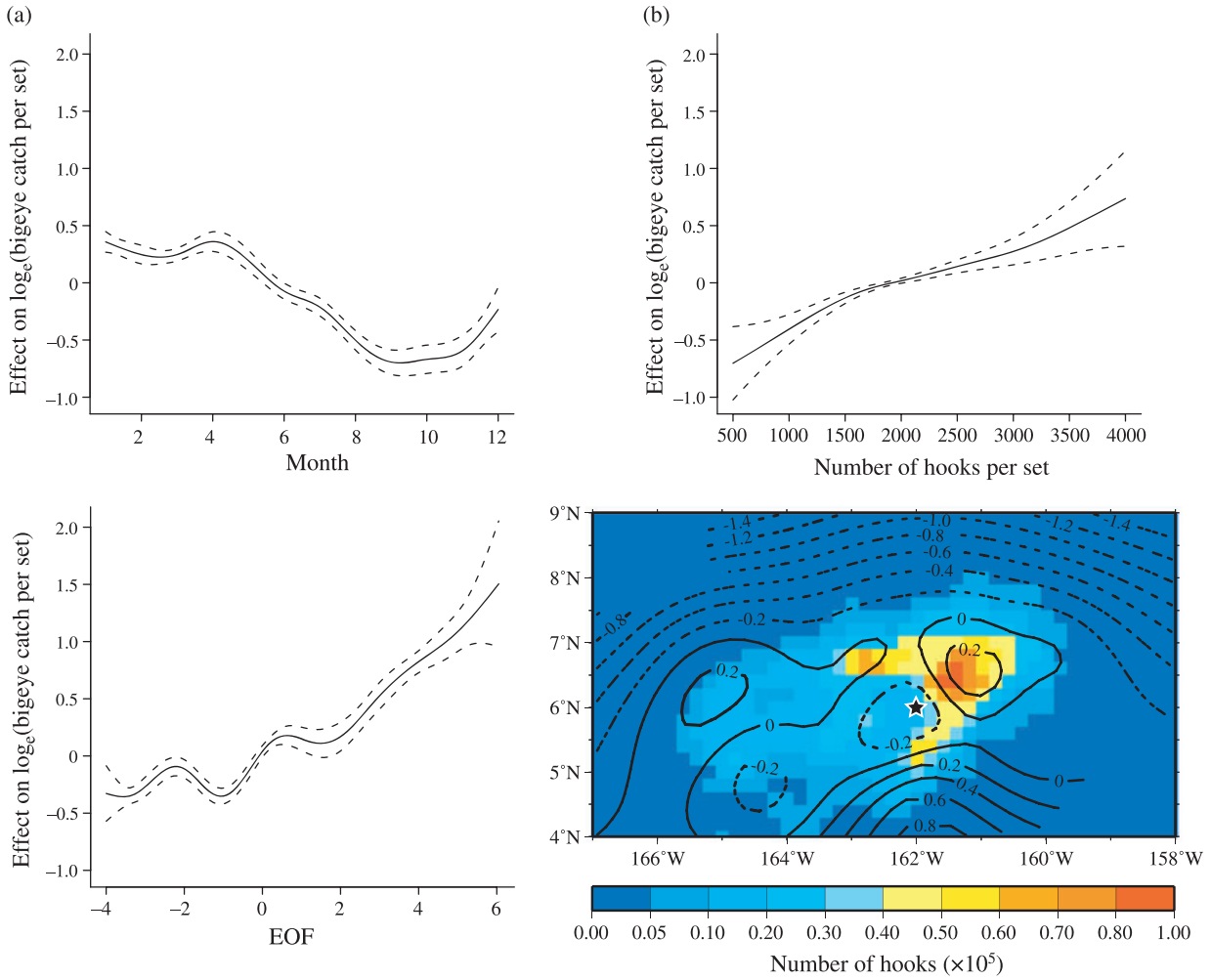

allowing a greater vertical range of habitat where other species may be limited by depth. The mechanisms that alter the subsurface environment may also affect the longline gear. A strong SSH gradient was present in the Palmyra region during the 1997–98 El Niño as seen in our EOF analysis. This gradient represented an increase in the geostrophic (subsurface) flow that may increase shoaling of longline sets, effectively placing the gear at shallower depths. Longline fisherman generally set their gear in a consistent configuration in this area, so environmental forcing on the gear may be important. Ecological factors such as predator avoidance may also be important during these times.

Figure 8. (a) The monthly aggregated correlations between the GAM-predicted bigeye catch per set and the logbook-observed bigeye values. (b) A quantile–quantile plot of the monthly aggregated observed bigeye and model predicted bigeye catch per set. The black line represents a 1 : 1 line of equivalence.

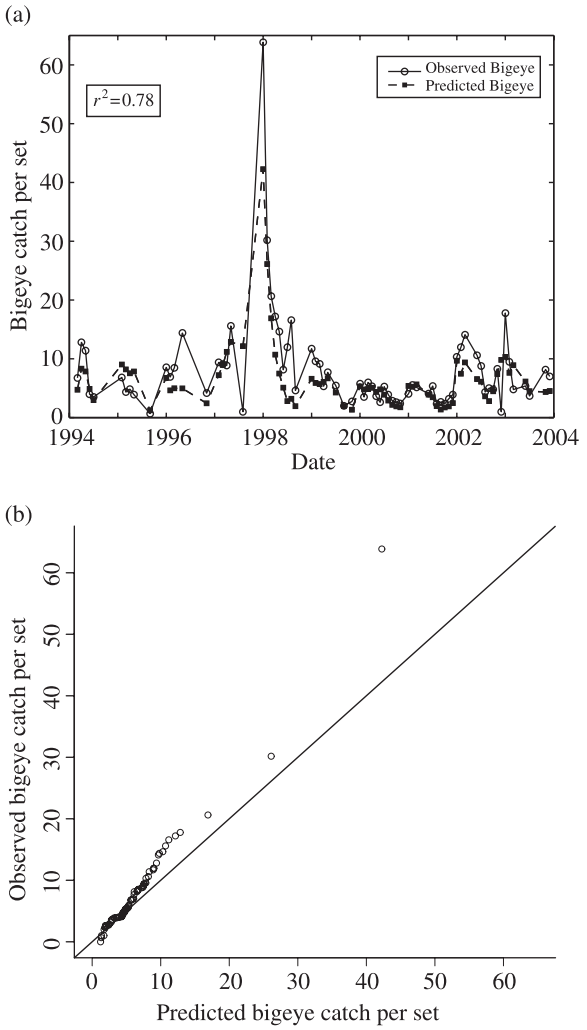

Horizontal shifts in distribution or habitat may also explain enhanced catch rates during El Niño events. A reversal in the overall transport of the surface layer and subsurface layer below the thermocline at the equator was also observed during this El Niño event (Johnson and McPhaden, 2000). Transport was eastward for both layers from the boreal spring through boreal fall 1997, reversing westward in boreal spring 1998 until boreal fall 1998. A preferred habitat based on temperature or forage may then be advected east with this horizontal shift in transport. Tagging studies of skipjack tuna showed west to east movement during the 1991–92 El Niño event (Lehodey *et al.*, 1997). These results were also observed by modeling the movement of skipjack forage during El Niño events (Lehodey *et al.*, 1998). Although, skipjack tuna are generally caught in depth ranges less than 100 m (Boggs, 1992) they may be used here to illustrate the mechanism for lateral migration of bigeye tuna in El Niño events. A consolidation of prey assemblages in this region from strong currents and eddy activity may increase the residence time of bigeye in this region.

One inherent problem in the longline logbook data is the absence of basic biological information such as fish length, weight, or sex. This makes it difficult to decipher the exact mechanisms for this increase in bigeye catch rates during El Niño events. Size or weight distribution data could provide insight as to the composition of age structure, separating the adult bigeye from new recruits in the area. While the logbook data lacks such information, there are other sources of size information such as the longline vessel observer program and auction/dealer reports. However, for the year of interest (1998) there was <5% observer coverage in the Palmyra region, with too few fish measured for meaningful comparisons. Auction/dealer reports contain aggregated landing summaries from a particular trip, and fish from individual sets are not tracked in the data; hence, auction/dealer reports are of limited use in mapping size distributions over time and space. Current observer coverage is 20–40%, and we eagerly look forward to examining bigeye size structure with the next El Niño event.

There may also be an increase in catch rates due to greater efficiency of the vessels since 1994. Effort increased substantially in 1998 as vessels began to target tuna species instead of swordfish, resulting in completely different gear assemblages and placement. Experience and enhanced knowledge of the fishing grounds over time would also result in a rise in efficiency, yet this may be offset by strong El Niño events which would form anomalous environmental conditions and alter gear placement.

The area around Palmyra Atoll represents a small part of the Hawaii Longline Fishery yet accounts for a large percentage of the bigeye caught in this fishery. The importance of catch variability for this reason is clear, but the placement of this study in a larger frame is somewhat difficult. If we use CPUE values as a proxy for abundance, then the large increase during 1998 would be indicative of a larger population structure across the equatorial band. Conversely, if the increase in CPUE did not correspond to an overall increase in population, this would result in an increase of the removal of bigeye from the system. If the bigeye population in this region is composed of new recruits

from the western waters then this would result in a decrease in available recruits to the equatorial system.

Our final model is based on one temporal, one interactive spatial, and one environmental parameter to facilitate analysis of term importance. Preliminary runs incorporated a lunar index based on the moon phase when the fishing gear was set, but this variable was found to be statistically unimportant ($P = 0.22$) and did not significantly improve the model fits. The bottom depth at the fishing gear location was also incorporated into preliminary runs but was also discarded for insignificance ($P = 0.24$). The longline set month predictor showed the seasonal effect on bigeye catch rates throughout the year with higher catch rates from December through April. The dependence on spatial location was modeled as a bivariate function of longitude and latitude. This provides a two-dimensional representation of the areas of highest effect on bigeye catch rates which is preferred over modeling the spatial effect as two additive univariate functions to avoid potential loss of information. The spatial effect shows that the areas northeast and northwest of Palmyra Atoll had the highest effect on catch rates. Both of these areas were centered between 6 and 8°N, an area of high eddy variability and current reversals. This supports the hypothesis that it is more a zonal effect than a meridional one as the reversal in currents during El Niño events is during December–April in that latitudinal band.

Work by Holland *et al.* (1990) illustrated the effects that fish aggregating devices (FADs) had on bigeye tuna. Extrapolating this idea further, the area around Palmyra Atoll can be considered as a large seamount. This feature may attract the migrating bigeye tuna and form an advantageous forage area during the times of enhanced flow and current reversal. The spatial effect also locates an area of high catch to the south of Palmyra Atoll. The increasing values directly to the south lie over an area of low historical effort and may be an artifact of small sample size. The model breaks apart the fishery-dependent, temporal, and environmental effects to assess the impacts of each predictor, and explains 36% of the cumulative deviance. Intra and interannual variability were the most important predictors in the model, which resulted in the inability to fit sets with very low or very high catch values. The model predicted sets with little or no catch, which occurred during an El Niño or early in the year as higher values, resulting in the deviations from the 1 : 1 line of equivalence seen in the Q–Q plot of the monthly data. Conversely, the model has difficulty with sets of very high catch regardless of time or space. Attempts to tune the model to fit these higher sets resulted in a larger deviation in the lower or zero catch sets. Additional environmental parameters such as the mean eastward velocity with 3- and 6-month lags were modeled, but resulted in a marginal increase in cumulative deviance explained while increasing the residuals for lower catch sets. This data set spanned two moderates and one strong El Niño event. Additional collection during future El Niño events with enhanced data including size and sex will further allow us to understand the variability in bigeye catch rates of this small, productive region of the Pacific.

In conclusion, observations from environmental data combined with the results from a GAM indicate that El Niño events have a positive influence on the catch rates of bigeye tuna around the Palmyra Atoll. El Niño triggers an eastward expansion of the warm pool waters along the equator, with a shoaling of the thermocline north of 5°N. This eastward advection and resulting reversal in flow, coupled with vertical changes in habitat, appears to increase the availability of bigeye tuna to the longline fishery.

ACKNOWLEDGEMENTS

The authors wish to thank William Walsh, Walter Machado, and Jerry Wetherall for reading and commenting on early drafts of this manuscript and Judith Kendig of the editorial staff of the Pacific Islands Fisheries Science Center (PIFSC) for help in preparation of this manuscript. We also wish to thank Marti McCracken for statistical consultation and her help in finalizing the GAM experimental design. The authors also wish to thank Peter Ward, Ian Perry, and an anonymous reviewer for their helpful comments. Jeffrey Polovina also made helpful contributions towards the final manuscript. Altimetry data used in this study were produced by the Ssalto program and obtained from Collecte Localization Satellites (CLS) center under the auspices of the Centre National d'études Spatiales of France (CNSF). TAO buoy data were produced by the TAO project at the Pacific Marine Environmental Laboratory (PMEL). The Hawaii Longline Logbook data were provided by the Fisheries Monitoring and Socio-economics Division at the Pacific Islands Fisheries Science Center.

REFERENCES

Bigelow, K.A., Boggs, C.H. and He, X. (1999) Environmental effects on swordfish and blue shark catch rates in the US North Pacific longline fishery. *Fish. Oceanogr.* **3:**178–198.

Bigelow, K.A., Hampton, J. and Miyabe, N. (2002) Application of a habitat-based model to estimate effective longline fishing effort and relative abundance of Pacific bigeye tuna (*Thunnus obesus*). *Fish. Oceanogr.* **11:**143–155.

Boggs, C.H. (1992) Depth, capture time, and hooked longevity of longline-caught pelagic fish: Timing bites of fish with chips. *U.S. Fish. Bull.* **90:**642–658.

Brill, R.W. (1994) A Review of temperature and oxygen tolerance studies of tunas pertinent to fisheries oceanography, movement models and stock assessments. *Fish. Oceanogr.* **3:**204–216.

Hanamoto, E. (1987) Effect of oceanographic environment on bigeye tuna distribution. *Bull. Jap. Soc. Sci. Fish Oceanogr.* **51:**203–216.

Harrell, F.E. (2001) *Regression Modeling Strategies with Applications to Linear Models, Logistic Regression, and Survival*. New York: Springer-Verlag, p. 545.

Hastie, T.J. and Tibshirani, R.J. (1990) *Generalized Additive Models*. London: Chapman & Hall, p. 335.

Holland, K.N., Brill, R.W. and Chang, R.K.C. (1990) Horizontal and vertical movements of yellowfin and bigeye tuna associated with fish aggregating devices. *U.S. Fish. Bull.* **88:**493–507.

Ito, R.Y. and Machado, W.A. (1999) Annual report of the Hawaii-based longline fishery for 1998. *NMFS/SWFSC Administrative Report* No. H-99-06, p. 62.

Johnson, G.C. and McPhaden, M.J. (2000) Upper equatorial Pacific Ocean current and salinity variability during the 1996-1998 El Niño-La Niña cycle. *J. Geophys. Res.* **105:**1037–1053.

Lehodey, P., Bertignac, M., Hampton, J., Lewis, A. and Picaut, J. (1997) El Niño Southern Oscillation and tuna in the western pacific. *Nature* **389:**715–718.

Lehodey, P., Andre, J.M., Bertignac, M. *et al.* (1998) Predicting skipjack tuna forage distributions in the equatorial Pacific using a coupled dynamical bio-geochemical model. *Fish. Oceanogr.* **7:**317–325.

Musyl, M.K., Brill, R.W., Boggs, C.H., Curran, D.S., Kazama, T.K. and Seki, M.P. (2003) Vertical movements of bigeye tuna (*Thunnus obesus*) associated with islands, buoys, and seamounts near the main Hawaiian Islands from archival data. *Fish. Oceanogr.* **12:**152–169.

Picaut, J., Ioualalen, M., Menkes, C., Delcroix, T. and McPhaden, M.J. (1996) Mechanism of the zonal displacements of the Pacific warm pool: implications for ENSO. *Science* **274:**1486–1489.

Polovina, J.J., Kleiber, P. and Kobayashi, D. (1999) Application of TOPEX/POSEIDON satellite altimetry to simulate transport dynamics of larvae of the spiny lobster (*Panulirus marginatus*), in the northwestern Hawaiian Islands, 1993–96. *U.S. Fish. Bull.* **97:**132–143.

Polovina, J.J., Howell, E.A., Kobayashi, D.R. and Seki, M.P. (2001) The transition zone chlorophyll front, a dynamic global feature defining migration and forage habitat for marine resources. *Prog. Oceanogr.* **49:**469–483.

Polovina, J.J. and Howell, E.A. (2005) Ecosystem indicators derived from satellite remotely sensed oceanographic data for the North Pacific. *ICES J. Mar. Sci.* **62:**319–327.

Swartzman, G., Huang, C. and Kaluzny, S. (1992) Spatial analysis of Bering Sea groundfish survey data using generalized additive models. *Can. J. Fish. Aquat. Sci.* **49:**1366–1378.

Uddstrom, M.J. and Oien, N.A. (1999) On the use of high-resolution satellite data to describe the spatial and temporal variability of sea surface temperatures in the New Zealand area. *J. Geophys. Res.* **104:**20729–20751.

Walsh, W.A. (2000) Comparisons of fish catches reported by fishery observers and in logbooks of Hawaii-based commercial longline vessels. *NMFS/SWFSC Administrative Report* No. H -00-07, p. 45.

Walsh, W.A. and Kleiber, P. (2001) Generalized additive model and regression tree analyses of blue shark (*Prionace glauca*) catch rates by the Hawaii-based commercial longline fishery. *Fish. Res.* **53:**115–131.

Walsh, W.A., Kleiber, P. and McCracken, M. (2002) Comparison of logbook reports of incidental blue shark catch rates by Hawaii-based longline vessels to fishery observer data by application of a generalized additive model. *Fish. Res.* **58:**79–94.

Wilson, C. and Adamec, D. (2001) Correlations between surface chlorophyll and sea surface height in the tropical Pacific during the 1997–1999 El Niño-Southern Oscillation event. *J. Geophys. Res.* **106:**31175–31188.

Wood, S.N. (2000) Modelling and smoothing parameter estimation with multiple quadratic penalties. *J. R. Stat. Soc. Bull.* **62:**413–428.

Wood, S.N. and Augustin, N.H. (2002) GAMs with integrated model selection using penalized regression splines and applications to environmental modelling. *Ecol. Model.* **157:**157–177.